Design of a Bragg fiber with large mode area for mid-infrared applications

Somnath Ghosh,[1,*] Sonali Dasgupta,[2] Ravi K. Varshney,[1] David. J. Richardson[2] and Bishnu P. Pal[1]

[1]*Indian Institute of Technology Delhi, Hauz Khas, New Delhi – 110016, India*
[2]*Optoelectronics Research Centre, University of Southampton, SO167FB, UK*
**somiit@rediffmail.com*

Abstract: The design of an all-solid, soft glass-based, large mode area Bragg fiber for effective single mode operation with mode effective area exceeding 1100 μm^2 across the wavelength range of 2 – 4 μm is reported. The design adopts a new strategy to induce large differential loss between the fundamental and higher order modes for effective single-mode operation within few tens of centimetres length of an otherwise multimode fiber. In addition to having the potential for the targeted application in high power laser delivery systems; complemented by a zero dispersion wavelength at 2.04 μm and rapidly developing mid-IR optical sources, the proposed fiber should also be attractive for generation of high power, single mode and less divergent supercontinuum light over this mid-IR window.

OCIS codes: (060.4005) Microstructured fibers; (060.2280) Fiber design and fabrication.

References and links

1. B. Guo, Y. Wang, C. Peng, H. L. Zhang, G. P. Luo, H. Q. Le, C. Gmachl, D. L. Sivco, M. L. Peabody, and A. Y. Cho, "Laser-based mid-infrared reflectance imaging of biological tissues," Opt. Express **12**(1), 208–219 (2004).
2. P. Werle, F. Slemr, K. Maurer, R. Kormann, R. Mucke, and B. Janker, "Near- and mid-infrared laser-optical sensors for gas analysis," Opt. Lasers Eng. **37**(2-3), 101–114 (2002).
3. A. B. Seddon, Z. Tang, D. Furniss, S. Sujecki, and T. M. Benson, "Progress in rare-earth-doped mid-infrared fiber lasers," Opt. Express **18**(25), 26704–26719 (2010).
4. J. Faist, F. Capasso, C. Sirtori, D. L. Sivco, A. L. Hutchinson, and A. Y. Cho, "Room temperature mid-infrared quantum cascade lasers," Electron. Lett. **32**(6), 560–561 (1996).
5. J. Faist, F. Capasso, C. Sirtori, D. L. Sivco, J. N. Baillargeon, A. L. Hutchinson, S. N. G. Chu, and A. Y. Cho, "High power mid-infrared (λ ~ 5 μm) quantum cascade lasers operating above room temperature," Appl. Phys. Lett. **68**(26), 3680–3682 (1996).
6. M. Lončar, B. G. Lee, L. Diehl, M. A. Belkin, F. Capasso, M. Giovannini, J. Faist, and E. Gini, "Design and fabrication of photonic crystal quantum cascade lasers for optofluidics," Opt. Express **15**(8), 4499–4514 (2007).
7. S. D. Jackson, A. Sabella, and D. G. Lancaster, "Application and development of high-power and highly efficient silica-based fiber lasers operating at 2 μm," IEEE J. Sel. Top. Quantum Electron. **13**(3), 567–572 (2007).
8. Q. Wang, J. Geng, Z. Jiang, T. Luo, and S. Jiang, "Mode-locked Tm-Ho fiber laser with a Sb-based SESAM," **CMK2,** OSA/ CLEO (2011).
9. D. G. Lancaster, A. Sabella, A. Hemming, S. Bennetts, and S. D. Jackson, "Power-scalable thulium and holmium fibre lasers pumped by 793 nm diode lasers," **WE5,** OSA/ASSP (2007).
10. J. Wu, Z. Yao, J. Zong, A. Chavez-Pirson, N. Peyghambarian, and J. Yu, "Single frequency fiber laser at 2.05 μm based on Ho-doped germanate glass fiber," Proc. SPIE **7195**, 71951K (2009).
11. M. E. Likhachev, S. L. Semjonov, M. M. Bubnov, E. M. Dianov, V. F. Khopin, M. Yu. Salganskii, M. A. Gurjanov, A. N. Gurjanov, R. Jamier, P. Viale, S. Fevrier, and J. M. Blondy, "Development and study of Bragg fibers with a large mode field and low optical losses," IEEE J. Quantum Electron. **36**(7), 581–586 (2006).
12. S. Février, R. Jamier, J. M. Blondy, S. L. Semjonov, M. E. Likhachev, M. M. Bubnov, E. M. Dianov, V. F. Khopin, M. Y. Salganskii, and A. N. Guryanov, "Low-loss singlemode large mode area all-silica photonic bandgap fiber," Opt. Express **14**(2), 562–569 (2006).
13. S. Février, P. Viale, F. Gerome, P. Leproux, P. Roy, J. M. Blondy, B. Dussardier, and G. Monnom, "Very large effective area singlemode photonic bandgap fiber," Electron. Lett. **39**, 1240–1242 (2003).

#150824 - $15.00 USD Received 11 Jul 2011; revised 8 Sep 2011; accepted 8 Sep 2011; published 12 Oct 2011

14. X. Feng, F. Poletti, A. Camerlingo, F. Parmigiani, P. Horak, P. Petropoulos, W. H. Loh, and D. J. Richardson, "Dispersion-shifted all-solid high index-contrast microstructured optical fiber for nonlinear applications at 1.55 microm," Opt. Express **17**(22), 20249–20255 (2009).
15. S. Dasgupta, B. P. Pal, and M. R. Shenoy, "Nonlinear spectral broadening in solid-core Bragg fibers," J. Lightwave Technol. **25**(9), 2475–2481 (2007).
16. H. T. Bookey, S. Dasgupta, N. Bezawada, B. P. Pal, A. Sysoliatin, J. E. McCarthy, M. Salganskii, V. Khopin, and A. K. Kar, "Experimental demonstration of spectral broadening in an all-silica Bragg fiber," Opt. Express **17**(19), 17130–17135 (2009).
17. P. Yeh, A. Yariv, and E. Marom, "Theory of Bragg fiber," J. Opt. Soc. Am. **68**(9), 1196–1201 (1978).
18. S. Dasgupta, B. P. Pal, and M. R. Shenoy, Chapter on Photonic bandgap guided Bragg fibers in Guided Wave Optical Components and Devices: Basics, Technology, and Applications, B. P. Pal (Ed.), Elsevier Academic Press, Burlington & San Diego (2006).
19. B. Temelkuran, S. D. Hart, G. Benoit, J. D. Joannopoulos, and Y. Fink, "Wavelength-scalable hollow optical fibres with large photonic bandgaps for CO2 laser transmission," Nature **420**(6916), 650–653 (2002).
20. Y. Fink, D. J. Ripin, S. Fan, C. Chen, J. D. Joannopoulos, and E. L. Thomas, "Guiding optical light in air using an all-dielectric structure," J. Lightwave Technol. **17**(11), 2039–2041 (1999).
21. X. Feng, A. K. Mairaj, D. W. Hewak, and T. M. Monro, "Nonsilica glasses for holey fibers," J. Lightwave Technol. **23**(6), 2046–2054 (2005).
22. X. Feng, T. M. Monro, P. Petropoulos, V. Finazzi, and D. J. Richardson, "Extruded single mode high-index core one-dimensional microstructured optical fiber with high index contrast for highly nonlinear optical deivces," Appl. Phys. Lett. **87**(8), 081110–081113 (2005).
23. P. Domachuk, N. A. Wolchover, M. Cronin-Golomb, A. Wang, A. K. George, C. M. B. Cordeiro, J. C. Knight, and F. G. Omenetto, "Over 4000 nm bandwidth of mid-IR supercontinuum generation in sub-centimeter segments of highly nonlinear tellurite PCFs," Opt. Express **16**(10), 7161–7168 (2008).
24. G. Brambilla, F. Koizumi, V. Finazzi, and D. J. Richardson, "Supercontinuum generation in tapered bismuth silicate fibres," Electron. Lett. **41**(14), 795–797 (2005).
25. J. Hu, C. R. Menyuk, L. B. Shaw, J. S. Sanghera, and I. D. Aggarwal, "Generating mid-IR source using $As_2 S_3$-based chalcogenide photonic crystal fibers," **CThN6,** OSA/CLEO/IQEC (2009).
26. G. Genty, T. Ritari, and H. Ludvigsen, "Supercontinuum generation in large mode-area microstructured fibers," Opt. Express **13**(21), 8625–8633 (2005).
27. K. Thyagarajan, R. K. Varshney, P. Palai, A. K. Ghatak, and I. C. Goyal, "A novel design of a dispersion compensating fiber," IEEE Photon. Technol. Lett. **8**(11), 1510–1512 (1996).

1. Introduction

Applications such as gas sensing for security and environmental monitoring, spectroscopy for pollution monitoring, industrial process control and astronomy have become increasingly important in recent years [1–3]. Much progress in these areas relies on the development of lasers and laser delivery systems that can efficiently emit and transmit light at mid-infrared (mid-IR) (2-20 μm) wavelengths. This has generated widespread interest in developing optical fibers that can enable efficient distortion-free transmission of optical signals at high power levels in the mid-IR to complement the design of efficient mid-IR optical sources such as high power Thulium/ Holmium doped fiber lasers and quantum cascade lasers operating at room temperatures [4–10]. Single-mode, large-mode area (LMA) fibers are crucial in this regard because they mitigate the undesirable nonlinear processes (e.g. stimulated Brillouin scattering, stimulated Raman scattering, four-wave mixing, etc.) in the fiber that deteriorate their power handling capability and thereby offer a better output beam quality. Single-mode LMA fibers based on step index profiles are limited in functionality due to their high bend-loss sensitivity and tight tolerances in fabrication parameters [11]. Thus, more recently, alternative routes have been explored that rely on the use of multimode LMA fibers in which effective single-mode guidance of the fundamental mode (FM) is achieved by inducing a large differential loss to its higher order modes (HOMs) [12,13]. The necessary differential loss is attained by engineering the fiber structure to control the inherent modal confinement loss and/or relative bend loss of the modes. Most of these designs are based on microstructured optical fibers (MOFs) that offer exceptional structural design freedom and control over the optical propagation characteristics. In this context, all-solid Bragg fiber, which is an example of 1D-photonic bandgap fiber, is extremely promising as it enables better control over the structural parameters with minimal transverse deformations during fiber drawing, thereby ensuring good repeatability of the structure [14–16]. Confinement of

#150824 - $15.00 USD Received 11 Jul 2011; revised 8 Sep 2011; accepted 8 Sep 2011; published 12 Oct 2011

light in these fibers occurs due to the photonic bandgap created by the periodic layers of alternating high and low refractive index (micrometer-thick) cladding layers [17, 18]. Bragg fibers can also provide considerably lower bending losses as compared to MOFs (with air holes) with same size of mode field [11] and have even been reported to negotiate 90° bends [19] without suffering bend-induced losses [20].

In this paper, we report a new design route to engineer the bandgap of a soft-glass based all-solid LMA Bragg fiber to achieve effective single-mode operation in the mid-IR wavelength region beyond 2 μm. Operating at these wavelengths necessitates the use of glasses other than silica (lead-silicate glasses in the case of this paper) that exhibit good transparency at these wavelengths [21] while having low toxicity, higher thermal stability and a mature fabrication process [22]. The proposed design strategy enables us to introduce a large differential loss of almost three orders of magnitude between the FM and HOMs as compared to existing designs of similar mode area [12, 13]. The proposed low-index-core fiber has five cladding layers and supports the LP_{01} mode with an average effective mode area of more than 1100 μm^2 over the operating wavelength range of 2–4 μm. Although the fiber is essentially multimoded at these wavelengths, we show that effective single-mode guidance can be established within few tens of centimetres of the fiber length, making it an attractive platform for high power (CW or short pulse) delivery as well as for generation of clean supercontinuum at relatively high powers [23–26] in the mid-IR.

2. Fiber design

It is well known that a Bragg fiber with a finite cladding is a leaky optical waveguide [17,18]. This feature has been gainfully exploited through judicious fiber design to guide the low-loss FM while allowing the HOMs with much larger losses to leak out [12]. The loss of the first higher order LP_{11} mode usually determines the length of the fiber that is required to make it effectively single-moded. The losses of the other core-guided HOMs are typically orders of magnitude higher and hence, they are lost from the core within a short length of the fiber. Here, we propose a novel design strategy that is based on choosing the cladding layers to be anti-resonant for the LP_{11} mode while simultaneously reflecting back the FM constructively into the core. This is in contrast to the more commonly used low-loss criterion for the FM [17, 18]. Since the HOMs extend farther into the cladding (as compared to the FM), the effect of the anti-resonant cladding on the HOMs is much stronger. In addition to the cladding, we design the core of the proposed fiber to be out of resonance with the LP_{11} mode, which increases its confinement loss while having a negligible impact on the confinement of the FM. Thereafter the number of cladding rings and the refractive index of the outermost ring are chosen to achieve the desired differential confinement loss. Table 1 shows the phase accumulated by the LP_{01} and LP_{11} modes in the core and the cladding, and demonstrates how the choice of the core and cladding widths preferentially leaks away the first HOM. In the wave-vector space, the choice of the core and cladding dimensions ensures that the transverse wave vector of the FM still lies well within the photonic bandgap while the wave vector of the LP_{11} mode and other HOMs lie close to the band edge. The underlying principle, which governs these features, exploits the following quarter wave stack condition for the LP_{01} mode:

$$k_1^0 d_1 = k_2^0 d_2 = \frac{\pi}{2} \tag{1}$$

where $k_i^0 = k_0\sqrt{(n_i^2 - n_{eff}^{0\ 2})}$; $i = 1, 2$, and n_{eff}^0 corresponds to the effective index of the LP_{01} mode while the following condition is satisfied for the LP_{11} mode along with its anti-resonant core:

$$k_1^1 d_1 = k_2^1 d_2 = \pi \tag{2}$$

#150824 - $15.00 USD Received 11 Jul 2011; revised 8 Sep 2011; accepted 8 Sep 2011; published 12 Oct 2011

where $k_i^1 = k_0\sqrt{(n_i^2 - n_{eff}^{1\,2})}$; $i = 1, 2$; and n_{eff}^1 corresponds to the effective index of the LP_{11} mode. The material system chosen is based on two thermally compatible lead-silicate glasses: LLF1 (refractive index n_1 = 1.5232) and SF6 (refractive index n_2 = 1.7577) (at the wavelength of 2 μm). The state-of-the-art extrusion-based fiber fabrication technique for these glasses is mature enough to realize the pre-determined set of structural parameters to obtain the desired optical characteristics [22].

Table 1. Phase accumulated by the LP_{01} and LP_{11} modes in the designed Bragg fiber

Parameters	Phase accumulated by	
	LP_{01} mode (in unit of π)	LP_{11} mode (in unit of π)
$k_c r_c$	0.670	1.000
$k_1 d_1$	0.530	0.795
$k_2 d_2$	0.965	0.965

where k_j is defined as $k_j = k_j^0 (\text{or } k_j^1)$ for the LP_{01} (or LP_{11}) mode; j = 1, 2; and $k_c = k_2$. We have used the commercially available software Comsol® based on the finite element method (FEM) for obtaining the modal characteristics of the fiber. The perfectly matched layers (PML) surrounding the fiber structure were optimized to calculate the confinement loss of the fiber. Since the Bragg fiber is a leaky structure, it is found that the mesh element sizes and the dimensions of the PMLs are quite critical in order to obtain the accurate loss characteristics of the fiber. Thus, a convergence check was performed on the losses obtained for the designed fiber with various PML thicknesses and mesh element sizes.

3. Results and discussions

In order to study propagation characteristics of the designed fiber and to discuss the practical implications of the above mentioned design through a detailed modal analysis of the proposed fiber, we have analyzed the designed fiber structure with suitably chosen five cladding layers surrounding the large core. Figure 1 shows a schematic of the refractive index profile of the designed fiber. The outermost layer is assumed to be a high-index layer. Figure 2 shows the confinement loss spectrum of nearly 300 eigen modes of the fiber. To analyze this loss spectrum, we have classified the modes into three different classes namely Band-1, Band-2 and Band-3. It is evident from Fig. 2 that the fiber supports those modes whose losses are lower than or comparable to that of the FM, which we have designated as Band-1 modes. Detailed investigations show that except for the FM, LP_{02} and LP_{21} modes, none of these modes are core guided. Rather these are modes that are actually guided by the high index cladding layers with very low fractional power in the core. Selective launch can be employed to ensure that the coupling efficiency into these high-index ring modes and the LP_{21} mode is negligible. The second category of modes, labeled as Band-2, encounters confinement loss ranging between 1 dB/m to 100 dB/m. This particular band consists of core guided modes with high differential confinement losses along with relatively smaller coupling efficiency,

#150824 - $15.00 USD Received 11 Jul 2011; revised 8 Sep 2011; accepted 8 Sep 2011; published 12 Oct 2011

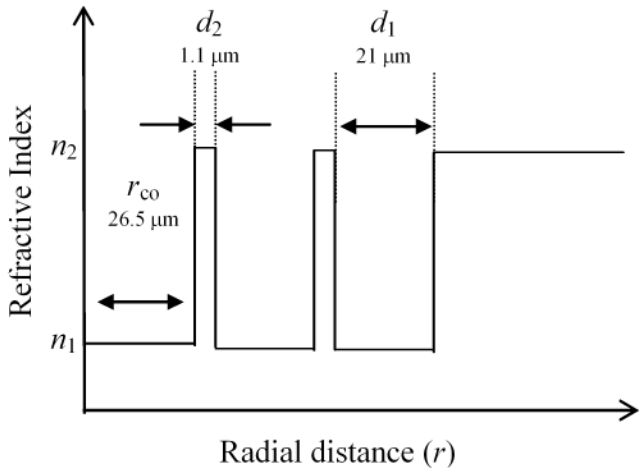

Fig. 1. Refractive index profile of the designed LMA Bragg fiber.

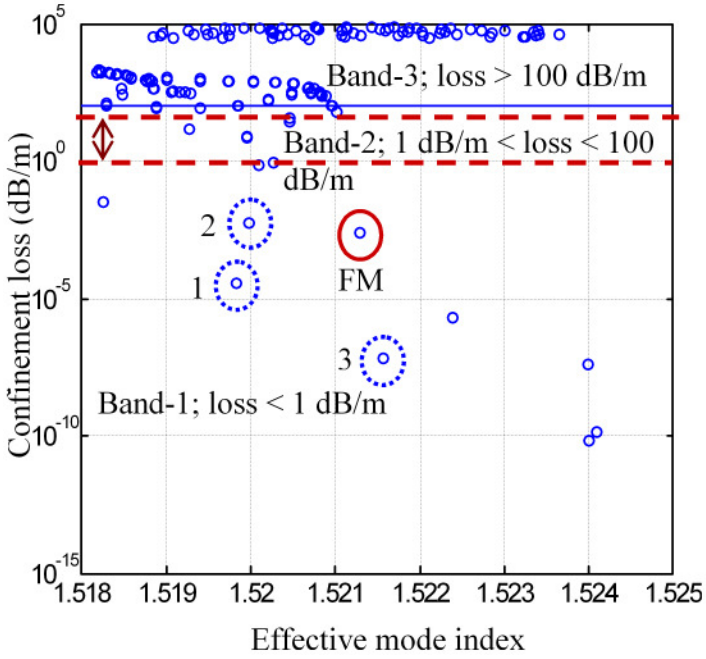

Fig. 2. Confinement loss spectrum as a function of mode effective index of the designed fiber (with five cladding layers) at the operating wavelength of 2.1 μm. Each dot on the graph corresponds to one eigen mode supported by the fiber geometry. The dot encircled in red is the FM. We have divided the modes into three categories. Band-1 modes: these are modes that exhibit confinement loss less than or ~1 dB/m. Except the FM, LP_{02} and LP_{21} modes, there is no core localized mode; Band-2 modes: these are modes with confinement loss ranging within 1 dB/m to 100 dB/m; Band-3 modes: modes with losses greater than 100 dB/m. LP_{11} mode falls within this category. Three sample modes in Band-1 have been encircled in dashed and marked as 1, 2 and 3. Their corresponding field distributions are shown in the top panel of Fig. 3.

which again favors losing them during propagation. Finally, the group of modes associated with confinement loss values more than 100 dB/m is designated as Band-3 modes. Since these modes experience losses as high as ~100 dB/m over the wavelength range of interest,

#150824 - $15.00 USD Received 11 Jul 2011; revised 8 Sep 2011; accepted 8 Sep 2011; published 12 Oct 2011

they would be lost within a very short length of the fiber and hence can be ignored for all practical purposes. Figure 3 shows the field distributions of three different randomly chosen modes corresponding to each of the three bands respectively. The top row of the figure which consists of a panel of three images clearly showed that the modes with losses less than that of the FM are the high-index ring modes (as shown Figs. 3a1, 3a2 and 3a3). These are the field distributions of the three randomly chosen modes encircled (in dashed) as 1, 2, and 3 in Fig. 2, respectively. The middle row displays the field distributions corresponding to modes with losses less than 100 dB/m, but localized within the core. As sample distributions, we have

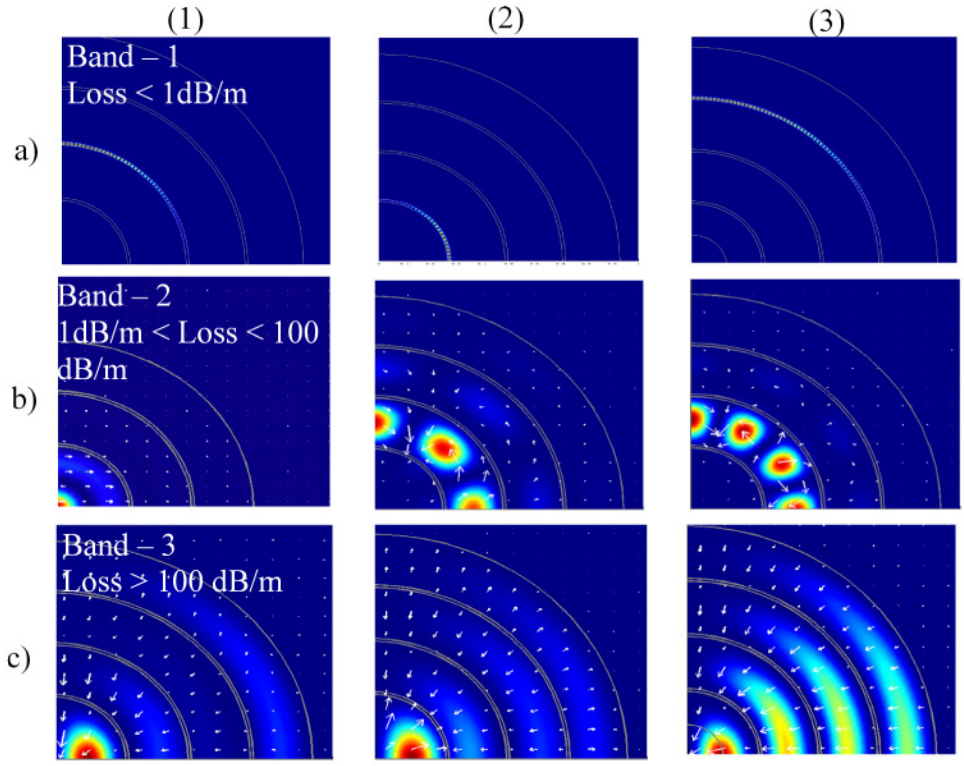

Fig. 3. Typical filed distributions of different categories of modes supported by the designed fiber. We have calculated the modes using a quarter structure of the fiber and employed various symmetry conditions to calculate all possible modes. The grey lines indicate the fiber geometry with PML. Arrows indicate the polarization state of the electric field. Figures 3a1) to 3a3) show the field distribution corresponding to the modes encircled as 1, 2, and 3, respectively in Fig. 2 under Band-1 modes. From these distributions it is clearly evident that these modes are not core guided modes. In Figs. 3b1) to 3b3) we have shown the field distributions corresponding to LP_{03}, LP_{31} and LP_{41} modes, respectively under the Band-2 modes. For the category of Band-3 modes, we have shown sample field distributions of LP_{11} (as Fig. 3c1) and two other HOMs of same symmetries (as Figs. 3c2 and 3c3).

displayed field distributions of LP_{03}, LP_{31} and LP_{41} as Figs. 3b1, 3b2, and 3b3, respectively.

The bottom row of Fig. 3 clearly depicts the signature of different HOMs with same symmetries as of LP_{11} mode. Figure 4 shows the confinement loss spectrum for the LP_{01} and LP_{11} modes demonstrating a large loss discrimination of more than three orders of magnitude between them across the entire wavelength range of 2 – 4 μm. The total (including the material loss) loss of the LP_{11} mode is ~100 dB/m over the proposed wavelength range, implying that a fiber length of ~25 cm will introduce a loss of ~25 dB to this mode, whereas the fundamental mode will suffer a total loss of less than 0.5 dB, which is essentially dominated by the much higher material loss (~2 dB/m) as compared to its confinement loss.

#150824 - $15.00 USD Received 11 Jul 2011; revised 8 Sep 2011; accepted 8 Sep 2011; published 12 Oct 2011

Thus, a length of 25 cm of the proposed LMA fiber will provide an essential effective differential loss of 20 dB between the LP_{01} and LP_{11} modes, which is sufficient to achieve effectively single-mode operation for high power delivery at wavelengths between 2 - 4 μm.

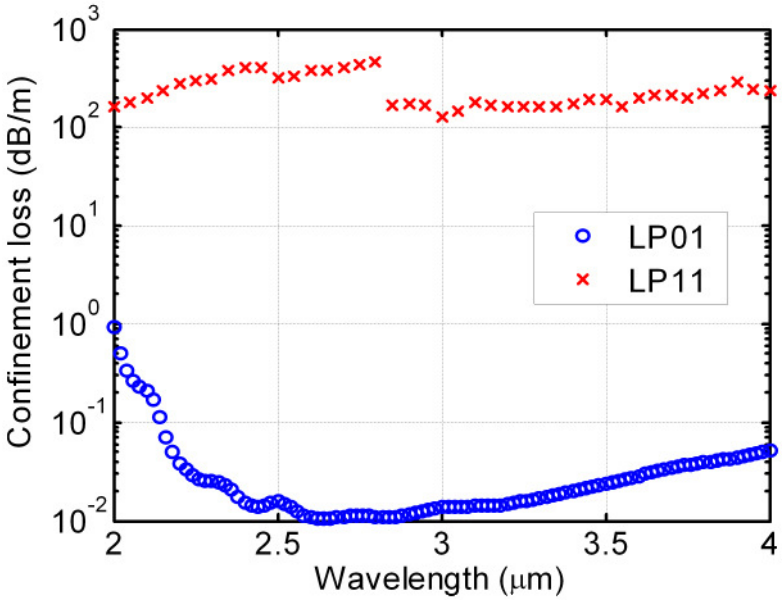

Fig. 4. Spectral response of the confinement loss of the FM and LP_{11} mode of the designed fiber.

We would like to point out that the core of the designed fibre does support the LP_{02} mode which exhibits a minimum confinement loss of more than 1dB/m across the operating wavelength range as shown in Fig. 5. Since the LP_{02} mode has the same symmetry as the FM, it would also be excited along with the FM (although all other supported modes will leak out from the proposed length of the designed fiber), thereby making the fiber dual-moded.

#150824 - $15.00 USD Received 11 Jul 2011; revised 8 Sep 2011; accepted 8 Sep 2011; published 12 Oct 2011

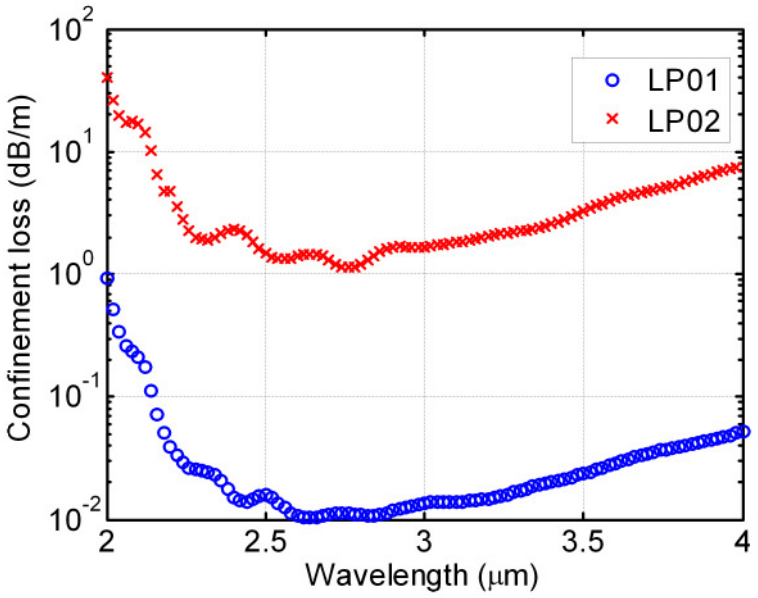

Fig. 5. Confinement loss spectrum of the LP_{02} mode as compared to the FM of the designed fiber.

Interestingly, the loss of this mode, which is more than 1 dB/m, is still two orders of magnitude higher than that of the FM (as shown in Fig. 5). Hence, with improvements in glass purity, the bulk loss of silicate glasses expected to go down to ~0.1 dB/m in the near future, and subsequently this differential loss being sufficient to enable modal discrimination, effective single-mode guidance is a distinct possibility. The discrimination could be further improved by exploiting the higher bend sensitivity of the HOMs and relatively larger fractional power content of the fundamental mode. Moreover, selective excitation of the LP_{01} mode by tapering the input end of the designed fiber could also be an alternative route towards better mode quality of the output beam [27].

Besides modal losses, the effective mode area is the other important characteristic parameter that limits the power level in high power delivery systems and controls the efficiency of various nonlinear processes along the fiber length. Figure 6 shows variation in effective area of the FM between 2 – 4 μm wavelengths. Note that the variation is extremely small across this entire wavelength range of interest and exhibits an average value of ~1100 μm^2. The inset in Fig. 6 shows the electric field distribution of the LP_{01} mode of the designed fiber at the operating wavelength of 2.1 μm, illustrating that the field is well-confined within the core. Even though the nonlinearity of the chosen lead silicate glasses (fiber core (n_2) ~2×10^{-19} m^2/W) is ~10 times higher than that of silica, the large mode area of the proposed fiber yields an effective nonlinearity of ~0.5 $(W. Km)^{-1}$, which is comparable to a standard silica fiber of much smaller effective mode area. Hence, the nonlinear effects that are detrimental for high power delivery would be considerably suppressed in the proposed LMA fiber in spite of the fiber material's higher nonlinearity than conventional silica fibers.

#150824 - $15.00 USD Received 11 Jul 2011; revised 8 Sep 2011; accepted 8 Sep 2011; published 12 Oct 2011

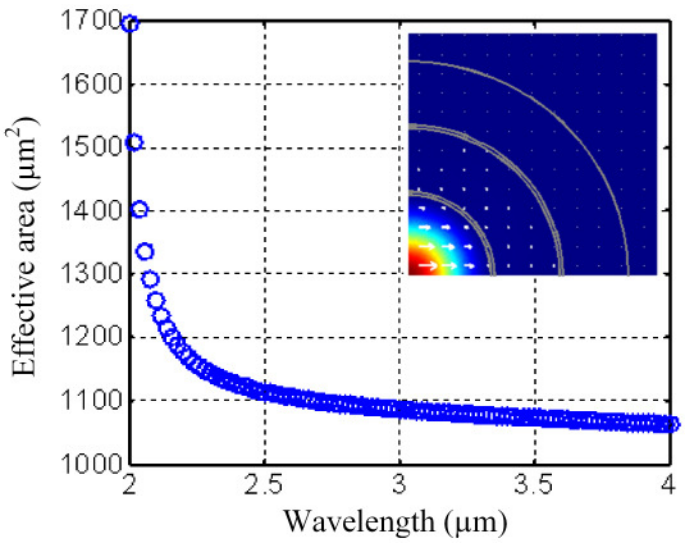

Fig. 6. Variation of effective area of the FM with wavelength. Inset shows the field profile of the FM in one-quarter of the fiber structure at λ = 2.1 μm. The grey lines indicate the fiber geometry. Arrows indicate the polarization state of the electric field.

We have also investigated the tolerance performance of the proposed fiber design with respect to deviations in the cladding layer thicknesses. It was observed that variations of up to ± 5% in the cladding layer thickness do not significantly alter the propagation characteristics of the relevant modes. Due to its all-solid large core geometry with five cladding layers, fabrication of such a fiber should be easily achievable through the extrusion process [14, 22]. Bigger core size and sufficiently thick cladding layers should also enable better control during fabrication and prevent any birefringence of any form [26].

Figure 7 shows the total dispersion (including material and waveguide dispersion) spectrum calculated for the FM of the fiber. It has zero dispersion wavelength (ZDW) at 2.04 μm and a small dispersion slope of ~0.07 ps/(km.nm^2) at the central wavelength of 3 μm. Interestingly, the ZDW at 2.04 μm is ideal for optically pumping such a fiber with Thulium/ Holmium doped fiber lasers. Thus, these dispersion characteristics of the designed fiber in conjunction with the availability of high power fiber lasers for pumping implies that it also has the potential to generate a large mode area continuum with a low divergent (numerical aperture of the fiber ~0.035) output spanning across the mid-IR region. An interesting aspect of the proposed fiber is the close proximity of its ZDW to the pump wavelength; a characteristic that is typically difficult to attain in LMA fibers meant for the mid-IR region wherein material dispersion dominates over waveguide dispersion making it difficult to tailor the dispersion characteristics. Continuum generation using LMA fibers is particularly attractive for achieving high throughput power, which is difficult with small core fibers due to the limitations imposed by the damage threshold of the fiber material. From this point of view our proposed fiber design should be attractive.

#150824 - $15.00 USD Received 11 Jul 2011; revised 8 Sep 2011; accepted 8 Sep 2011; published 12 Oct 2011

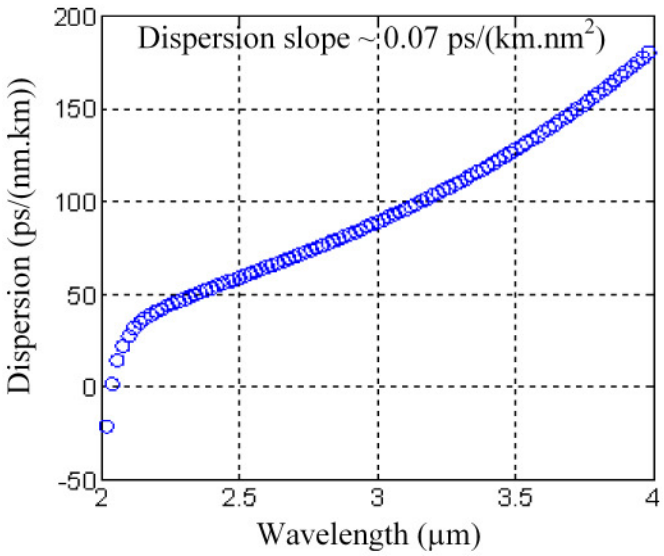

Fig. 7. Dispersion spectrum of the FM.

4. Conclusions

We have presented a novel design strategy to achieve large modal loss discrimination between the FM and the HOMs in a soft glass-based LMA Bragg fiber. We have shown that a such a fiber with as small as 25 centimeters of length would be sufficient to attain effective single-mode guidance across the wavelength range of 2 - 4 μm with an almost constant effective area of the FM exceeding 1100 μm^2. Combined with its zero dispersion wavelength at 2.04 μm, which is ideal for pumping with high-power Thulium-doped fiber lasers, the proposed fiber should be a promising candidate for high power delivery applications as well as SC generation at mid-infrared wavelengths.

Acknowledgments

This work is supported by the ongoing UK-India Education and Research Initiative (UKIERI) collaboration project. SG gratefully acknowledges his Pre-doctoral graduate student level exchange visit to the ORC under this project. SDG thanks Francesco Poletti at the ORC for helpful discussions on the modal characteristics of the fiber.

#150824 - $15.00 USD Received 11 Jul 2011; revised 8 Sep 2011; accepted 8 Sep 2011; published 12 Oct 2011